



Epigenetic profiling of the antitumor natural product psammaplin A and its analogues

José García^a, Gianluigi Franci^{b,f}, Raquel Pereira^a, Rosaria Benedetti^{b,c,e}, Angela Nebbioso^b, Fátima Rodríguez-Barríos^a, Hinrich Gronemeyer^d, Lucia Altucci^{b,f,*}, Angel R. de Lera^{a,*}

^a Departamento de Química Orgánica, Universidad de Vigo, 36310 Vigo, Spain

^b Dipartimento di Patologia generale, Seconda Università di Napoli, Vico L. De Crecchio 7, 80138 Napoli, Italy

^c Università di Napoli Federico II, Dipartimento di Chimica Organica e Biochimica, Italy

^d Department of Cancer Biology - Institut de Génétique et de Biologie Moléculaire et Cellulaire (IGBMC)/CNRS/INSERM/ULP, BP 163, 67404 Illkirch Cedex, C. U. de Strasbourg, France

^e Università di Napoli Federico II, Dipartimento di Fisica, 6, CNR-IGB, Via P. Castellino, 80100, Napoli, Italy

^f CNR-IGB, Via Pietro Castellino 80100 Napoli, Italy

ARTICLE INFO

Article history:

Received 30 September 2010

Accepted 8 December 2010

Available online 15 December 2010

Keywords:

Psammaplin A

Epigenetics

HDAC

DNMT

Total synthesis

Natural products

ABSTRACT

A collection of analogues of the dimeric natural product psammaplin A that differ in the substitution on the (halo)tyrosine aryl ring, the oxime and the diamine connection has been synthesized. The effects on cell cycle, induction of differentiation and apoptosis of the natural-product inspired series were measured on the human leukaemia U937 cell line. Epigenetic profiling included induction of p21^{WAF1}, effects on global H3 histone and tubulin acetylation levels as well as in vitro enzymatic assays using HDAC1, DNMT1, DNMT3A, SIRT1 and a peptide domain with p300/CBP HAT activity. Whereas the derivatives of psammaplin A with modifications in the length of the connecting chain, the oxime bond and the disulfide unit showed lower potency, the analogues with changes on the bromotyrosine ring exhibited activities comparable to those of the parent compound in the inhibition of HDAC1 and in the induction of apoptosis. The lack of HDAC1 activity of analogues modified on the disulfide bond suggests that its cleavage must occur in cells to produce the monomeric Zn²⁺-chelating thiol. This assumption is consistent with the molecular modelling of the complex of psammaplin A thiol with h-HDAC8. Only a weak inhibition of DNMT1, DNMT3A and residual activities with SIRT1 and a p300/CBP HAT peptide were measured for these compounds.

© 2010 Elsevier Ltd. All rights reserved.

1. Introduction

Psammaplin A (1, PsA, Scheme 1) is a symmetrical disulfide dimer derived from the condensation of modified tyrosine and cysteine units¹ (for a proposal of its biogenesis, see 2,3). Although it was first isolated in 1987 from an unidentified sponge⁴ and from *Psammaplysilla* sp.,^{5,6} PsA is found, together with biogenetically-related congeners, in several *Verongidas*^{2,3,6–10} and in some associations of these species.^{11,12}

Antibacterial and antitumor activities have been reported for PsA. The in vitro antibacterial activity of PsA against both *Staphylococcus aureus* (SA) and methicillin-resistant *Staphylococcus aureus* (MRSA) was considered the result of the inhibition of DNA gyrase¹³ and induced arrest of bacterial DNA synthesis. PsA also inhibits topoisomerase II (topo II),¹⁴ farnesyl protein transferase,⁸ leucine aminopeptidase,⁸ mycothiol-S-conjugate amidase,¹⁵ chitinase,¹⁰ Pol α -primase,¹⁶ PPAR γ ^{17–20} and mammalian aminopeptidase N

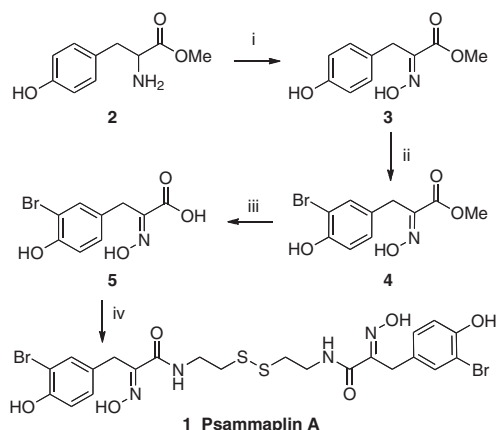
(APN).²¹ Targeting multiple proteins that impact on DNA topology, DNA replication, transcription, apoptosis, tumor invasion, and angiogenesis likely contributes to the significant cytotoxicity displayed by PsA in human lung (A549), ovarian (SKOV-3), skin (SK-MEL-2), CNS (XF498), and colon (HCT15) cancer cell lines.¹²

PsA was also reported to inhibit in vitro the chromatin-modifying enzymes histone deacetylase (HDAC) and DNA methyl transferase (DNMT).³ HDAC and DNMT are epigenetic enzymes that catalyze the covalent modifications of histone proteins and DNA in chromatin,²² and therefore they are considered prime new targets²³ for the treatment and prevention of cancer^{24–34} and other diseases.³⁵ The modification of chromatin is thus an addition to the list of potential mechanisms involved in the anticancer actions of the natural product PsA.

Histone acetylation is a dynamic process in which a cellular steady state is maintained by the opposing activities of histone acetyltransferases (HATs) and deacetylase enzymes (HDAC) acting at the ϵ -amino groups of evolutionally conserved lysine residues located at the histone N-termini. HATs transfer the acetyl moiety from acetyl CoA to the histone lysine residues whereas HDACs catalyze their removal. Individual HATs and HDACs display distinct

* Corresponding authors.

E-mail addresses: lucia.altucci@unina2.it (L. Altucci), qolera@uvigo.es (Angel R. de Lera).



Scheme 1. Reagents and conditions: (i) Na_2WO_4 , H_2O_2 , 25 °C, 3 h (63%); (ii) NBS, CH_3CN , 25 °C, 2 h (82%); (iii) LiOH, $\text{THF-H}_2\text{O}$, 23 °C, 12 h (99%); (iv) DCC, *N*-hydroxyphthalimide, Et_3N , cystamine, 1,4-dioxane, MeOH, 25 °C, 12 h (60%).

specificities for certain individual lysine residues and particular histones. Although the factors responsible for the specificity are poorly understood they might reflect different biological functions of the various enzymes. Regardless of the details, it is widely accepted that histone acetylation is essential to establish a transcriptionally competent state of chromatin²² and consequently contributes to the gene activation/gene repression transcriptional status of cells. Two histone deacetylase inhibitors (HDACis), suberoylanilide hydroxamic acid (SAHA, vorinostat, Zolinza[®]), and FK228 (romidepsin, Istodax[®]) are used as therapy for cutaneous T-cell lymphoma,³⁶ and several others are currently undergoing clinical trials as potential targeted cancer chemotherapeutic agents.^{37–41}

In eukaryotes DNMTs catalyze the addition of methyl groups from *S*-adenosyl-*L*-methionine (SAM) to the C5 position of cytosine bases within the CpG-rich islands in DNA. Methylation of DNA is an epigenetic mark associated to a repressed chromatin state which inhibits gene transcription.^{42,43} Several tumour suppressor genes are hypermethylated in tumours, which suggest a link between aberrant DNA methylation and cancer.^{44–47} DNA methyl transferase inhibitors (DNMTis)⁴⁸ structurally related to cytidine (5-azacytidine, Vidaza[®] and 5-aza-deoxycytidine, Dacogen[®]) are already in the clinic for the treatment of myelodysplastic syndrome.⁴⁹

Since histone acetylation and DNA methylation play a key role in the pathophysiology of cells, dual inhibitors of HDAC or DNMT are therapeutically more appealing than combination of these drugs.^{50,51} We thus became intrigued by the reports on the potent activity of psammaplin A (**1**) in the inhibition of these two epigenetic enzymes (HDAC: IC_{50} = 4.2 nM; DNMT: IC_{50} = 18.6 nM using *in vitro* cell-free enzyme assays)³ as well as by the *in vitro* and *in vivo* inhibition of tumour growth induced by this natural product.²⁰ Despite the reports indicating some drawbacks for the development of **1** as a drug due to its poor physiological stability,^{15,21,52} we undertook the synthesis of a family of analogues with the aim to discover more potent and selective derivatives of **1** as well as to shed light into the mechanism of epigenetic inhibition by **1**. Apart from the work of Nicolaou focused on antibacterial activities, no structure–activity relationship studies of the anticancer activities of PsA analogues have been reported, which are necessary for an eventual lead optimization project within this class of modified tetrapeptides.

2. Chemistry. Synthesis of psammaplin A and derivatives

All previous synthetic approaches to **1** have focused on the final construction of the dimeric disulfide structure by condensation of

the corresponding carboxylic acid with the symmetrical diamine cystamine. Both Hoshino et al.⁵³ and Nicolaou et al.^{54,55} installed the oxime function after the synthesis of the corresponding pyruvic acid derived from *L*-tyrosine, in a sequence that afforded **1** in moderate overall yields. Nicolaou then screened in antibacterial assays a 3828-membered library of heterodimeric psammaplin A analogues¹⁵ obtained from symmetrical precursors by combinatorial scrambling via catalytically-induced disulfide exchange reactions. A recently described three-step (43% overall yield) synthesis of PsA **1** starts from the considerably more expensive and less versatile 4-hydroxyphenylpyruvic acid.⁵⁶

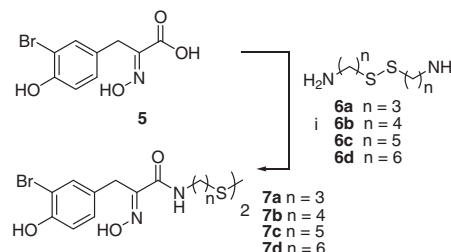
We modified the above synthesis of **1** by performing the bromination of the phenol ring on the corresponding oxime **3** (Scheme 1).⁵⁷ As shown on Scheme 1, the amino group of *L*-tyrosine **2** was oxidized to the hydroxyimino ester **3** in 60% yield using Na_2WO_4 and H_2O_2 in ethanol.⁵⁸ A monobrominated product **4** was obtained by treatment of **3** with one equivalent of NBS in CH_3CN at 25 °C,^{58,59} with no evidence of formation of the dibromo derivative or the dibrominated spirocyclic isoxazoline.⁵⁷ After saponification of **4** the carboxylic acid **5** was coupled with cystamine using Hoshino's conditions.⁵³ The overall yield for the synthetic sequence is 29%, with a slight improvement over the two routes previously described from *L*-tyrosine **2**. The synthetic scheme is advantageous for the preparation of diverse PsA analogues starting from commercial tyrosine derivatives.

Using the methodology depicted on Scheme 1, the synthesis of PsA homologues containing from three to six methylene units was completed, albeit in low yields (Scheme 2), using the non-commercial diamines **6a–d**, which were synthesized following a general methodology.⁶⁰

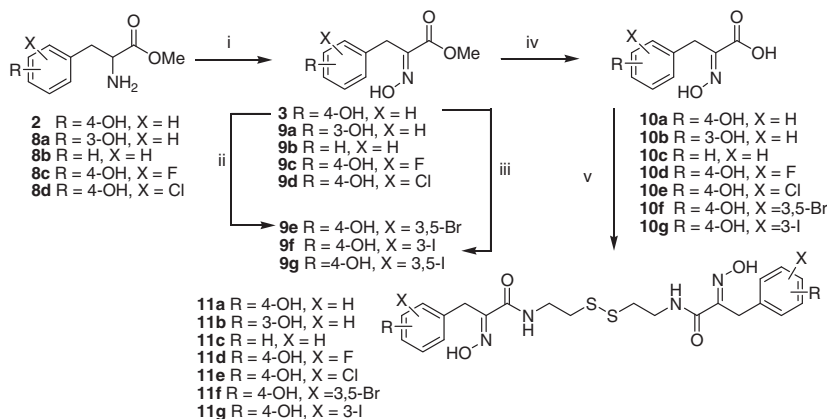
Similarly, PsA analogues that preserve the native connecting cystamine unit but differ in the substituents at the aryl ring (Scheme 3) were synthesized using either commercially available tyrosine derivatives or the synthetic halogenated analogues (with bromine or iodine at C3) after oxidation of the amine to the oxime (Scheme 3). Some compounds of the series (**11a**, **11c**, **11d** and **11e**) have previously been described by Nicolaou on his search for new antibacterial agents.⁵⁵ Bromopsammaplin A **11f** is also a natural product isolated from an association of the sponges *Jaspis wondensis* and *Poecillastra wondoensis*.¹²

Condensation of acid **5** with amines **12** and **14a–c** (Scheme 4) provided analogues **13** and **15a–c** which were designed to further our understanding of the mechanism underlying the biological activity of the parent PsA as HDAC inhibitor. The dimer **13** contains an ethylene group replacing the disulfide bond functionality. Products **15b,c** are monomers that have, respectively, methyl ether and methyl sulfide as end groups. The primary alcohol **16** was obtained by acidic (7:2:1 $\text{THF}/\text{HCO}_2\text{H}/\text{H}_2\text{O}$) deprotection of silyl ether **15a**.

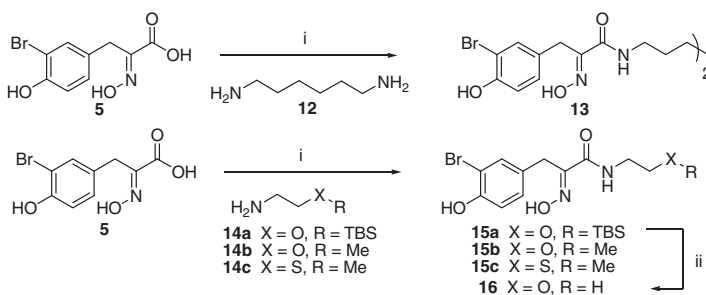
The derivative lacking the oxime was also of interest to reveal whether this functional group is critical for the epigenetic activity of **1**. Compound **20** was prepared as described on Scheme 5. The bromination of methyl 3-(4-hydroxyphenyl)propanoate using the



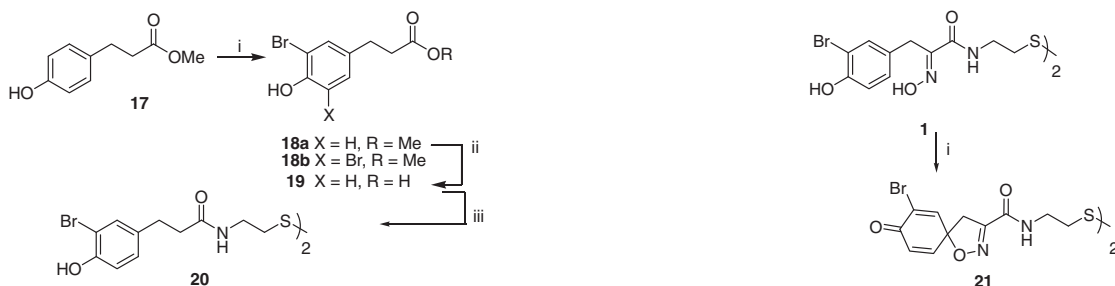
Scheme 2. Reagents and conditions: (i) DCC, *N*-hydroxyphthalimide, Et_3N , diamine **6**, 1,4-dioxane, MeOH, 25 °C, 12 h (**7a**, 16%; **7b**, 21%; **7c**, 34%; **7d**, 14%).



Scheme 3. Reagents and conditions: (i) Na_2WO_4 , H_2O_2 , 25 °C, 3 h (**9a**, 57%; **9b**, 50%; **9c**, 64%; **9d**, 80%); (ii) NBS, CH_3CN , 25 °C, 5 h (**9e**, 80%); (iii) I_2 , Ag_2SO_4 , MeOH, 25 °C, 15 min (**9f**, 51%; **9g**, 23%); (iv) LiOH, $\text{THF-H}_2\text{O}$, 23 °C, 12 h (**10a**, 99%; **10b**, 99%; **10c**, 99%; **10d**, 97%; **10e**, 98%; **10f**, 99%; **10g**, 99%); (v) DCC, *N*-hydroxyphthalimide, Et_3N , cystamine, 1,4-dioxane, MeOH, 25 °C, 12 h (**11a**, 46%; **11b**, 54%; **11c**, 15%; **11d**, 57%; **11e**, 57%; **11f**, 42%; **11g**, 52%).



Scheme 4. Reagents and conditions: (i) DCC, *N*-hydroxyphthalimide, Et_3N , **12** or **14a–c**, 1,4-dioxane, MeOH, 25 °C, 14 h (**13**, 70%; **15a**, 83%; **15b**, 20%; **15c**, 18%); (ii) 7:2:1 THF/ $\text{HCO}_2\text{H}/\text{H}_2\text{O}$, 25 °C, 14 h (76%).



Scheme 5. Reagents and conditions: (i) NBS, DMF, 25 °C, 5 h (**18a**, 56%; **18b**, 17%); (ii) LiOH, $\text{THF-H}_2\text{O}$, 23 °C, 12 h (99%); (iii) DCC, *N*-hydroxyphthalimide, Et_3N , cystamine, 1,4-dioxane, MeOH, 25 °C, 14 h (40%).

Scheme 6. Reagents and conditions: (i) MTA, CH_3CN , 25 °C, 15 h (5%).

conditions described for oxime **4** (NBS in CH_3CN) yielded a mixture of mono- and dibromo derivatives, **18a** and **18b**, respectively, in a 3:1 ratio. Hydrolysis of the former followed by the coupling of **19** with cystamine led to the desired disulfide **20** in moderate yield (Scheme 5).

Lastly the spirocyclic hexadienyl-isoxazoline **21**, a potential metabolite of PsA¹ could only be obtained, albeit in very low yield (5%), by the oxidative-induced cyclization⁶¹ of PsA **1** with manganese(III) tris(acetylacetonate) (MTA)⁶² (Scheme 6) after many other methods failed.

3. Biological characterization

Firstly, we focused on the reported inhibition of HDAC by PsA and the synthetic analogues, as well as on their effects on cell cycle, induction of differentiation and apoptosis on the U937 human

acute myeloid leukemia cell line. In vitro tests of the compounds at 5 μM on human recombinant HDAC1, using SAHA as a positive control, confirmed the enzymatic inhibition of PsA **1** (Fig. 1A). In addition, some analogues (**11a–e**, **11g**) reduced the activity of HDAC1 more efficiently than **1**. The other compounds of the series (**7a–d**, **11f**, **13**, **15b–c**, **16**, **20** and **21**) did not noticeably affect HDAC1 activity. Compounds with longer chain connecting the disulfide to the hydroxyimino amide (**7a–d**) lack significant inhibitory activity. A similar result was observed for compounds having the disulfide replaced by methylene units (**13**) and for the monomers with either methyl ether (–OMe), methyl thioether (–SMe) or alcohol (–OH) functionalities (**15b**, **15c** and **16**, respectively). In contrast, the inhibitory activity is maintained and even increased with compounds that preserve the general modified tetrapeptide scaffold of PsA regardless of the nature and pattern of the substituents at the aryl ring (**11a–f**). The more drastic change of the overall aryl ring structure imparted by the spirocycle together

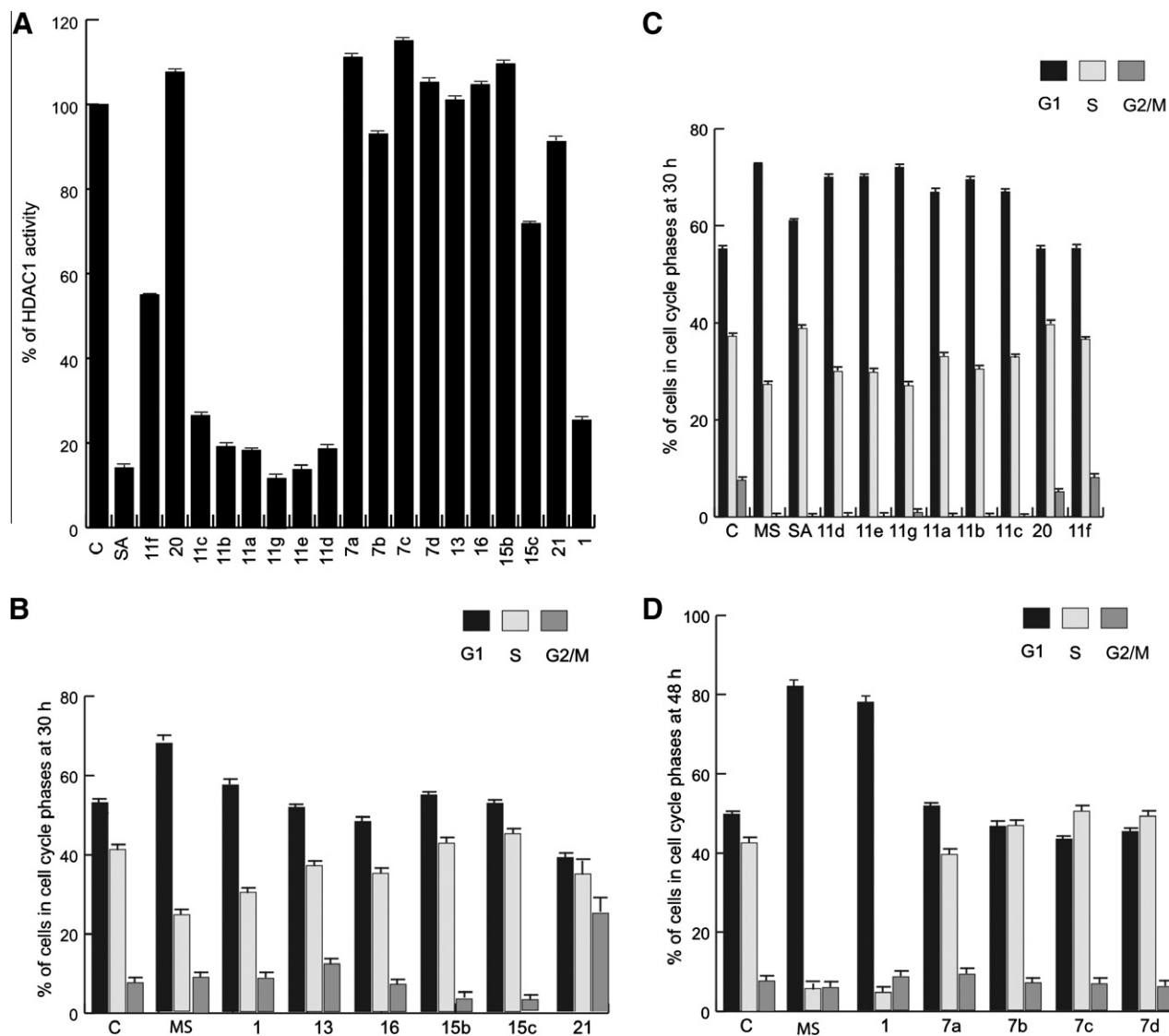


Figure 1. (A) HDAC1 fluorescent assay with the indicated compounds at 5 μ M. The inhibition is reported as percentage of activity relative to the control (100%). (B–D) Cell cycle analysis and apoptosis in U937 cells treated with the indicated compounds at 5 μ M for 30 h. The data represent the media of independent duplicates.

with the reduction of flexibility and the lack of free oxime in derivative **21** led to substantial loss of HDAC inhibitory activity.

Cell-based assays were performed on the U937 myeloid leukemia cells to determine the anti-proliferative potential and the ability of the compounds to revert myeloid tumor cells to differentiated granulocytes. Cell cycle progression, differentiation and amount of cells that undergo apoptosis following treatment with PsA **1** and analogues (5 μ M) for 30, 40, and 48 h were determined (Figs. 1B and 2). Compared to the vehicle-treated cells and relative to the positive control represented by the known HDACs MS275 (HDAC1,2,3-selective) and SAHA (also HDAC6 inhibitor),^{63,64} only PsA **1** and some analogues induced cell cycle arrest in G1 (Fig. 1, panels B–D). In particular after 30 h PsA induced a time-dependent accumulation of U937 cells in the G1 phase (60%), and analogues **11a–g** and **20** showed even greater arrest (80%), with values comparable to MS-275 (Fig. 1C). A clear correlation between the in vitro HDAC1 inhibition and the in vivo efficacy to induce cell cycle arrest was noticed for the most active compounds. Compound **21**, on the other hand, appears to block cell cycle at G2/M. The remaining analogues gave no detectable activities on cell cycle progression even after longer (48 h) treatment regimes (Fig. 1B and D).

The percentage of apoptotic cells (measured as caspase 3 activation by FACS analysis) increased when U937 cells were treated with **1** and series **11a–g** for 30 h (Fig. 2A). After 30 h induction with compounds **11a–e** and **11g** the percentage of apoptotic cells varied between 30% and 40%. Other compounds, including bromopsammaplin A (**11f**), and the derivative lacking the oxime function **20**, exhibited only minor effects even at longer incubation times (40 h). The results confirmed the in vitro findings since the most potent inducers of differentiation and apoptosis in U937 cells are the **11a–g** series of ring-modified PsA analogues (with the exception of bromopsammaplin A **11f**). Modifications in the chain length and the disulfide led to lower values of apoptosis, in agreement with the enzymatic assays. Interestingly, spiro derivative **21** showed comparable induction of apoptosis to parent **1**.

The differentiation of myeloid precursors to granulocytes was determined by measuring the presence on the cell membrane of the granulocytic differentiation marker CD11c antigen, which is highly expressed only on mature granulocytes, monocytes and certain lymphocytes, but not significantly on myeloid committed precursor cells. After treating the U937 cells with the PsA analogues at 5 μ M for 30 and 40 h, low differentiation levels

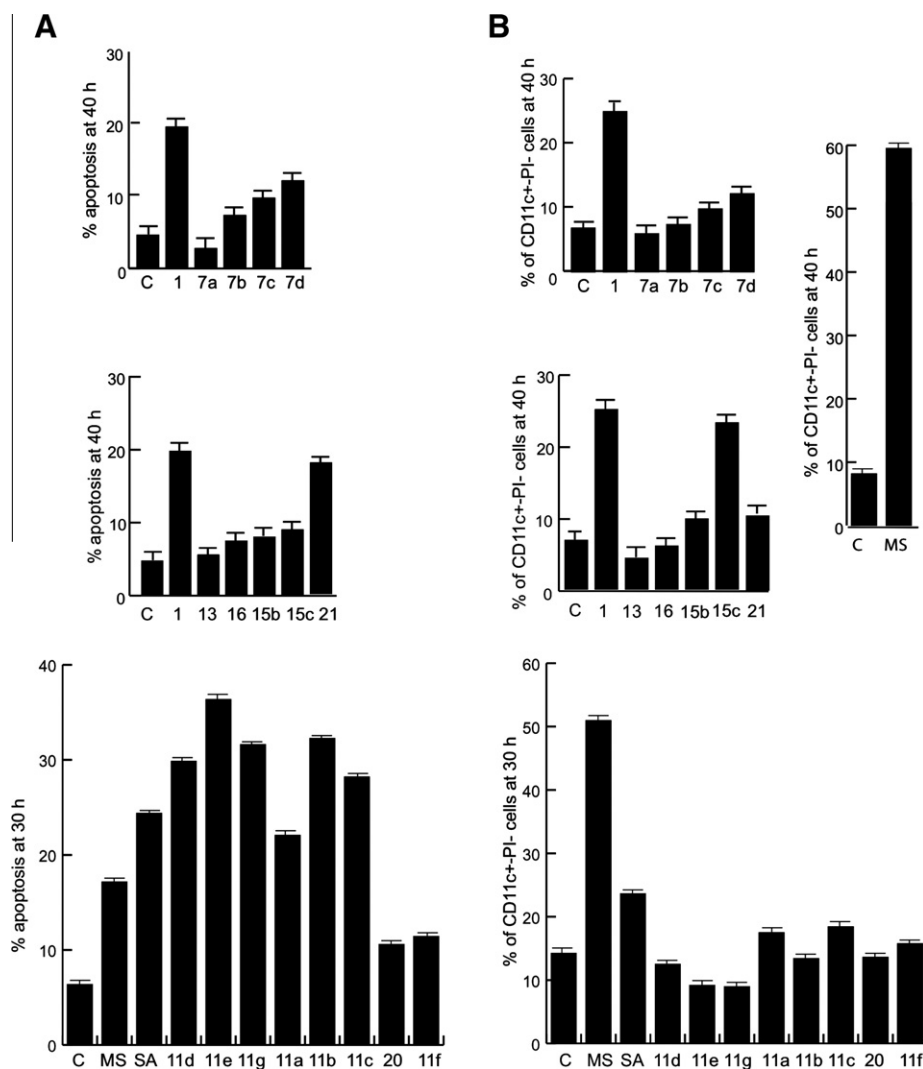


Figure 2. (A) Induction of apoptosis after treatment of U937 cells with the indicated compounds at 5 μ M, for 30 h (for the series **11a–11g**) and 40 h. (B) Differentiation analysis in U937 cells after 30 h treatment with the indicated compounds at 5 μ M. The percent value of CD11c positive/propidium iodide (PI) negative cells is represented. The data shown is the media of independent quadruplicates.

were measured (with the exception of parent **1** and methyl sulfide **15c**) relative to control (Fig. 2B) and to the class I-selective HDACi MS-275.

We next determined the expression levels of p21^{WAF1}, which is involved in the mechanism of tumor suppression, as well as the global acetylation status of histone (histone H3) and non-histone proteins (tubulin), that are substrates of HDACs family members. The up-regulation of p21^{WAF1} and the increase of tubulin acetylation levels were evaluated by Western blot analyses on total extracts after treating the U937 cells for 24 h with the compounds at 5 μ M (Fig. 3A–C). Compounds **7a–d**, **13**, **15b**, **16** and **21** failed to increase both p21^{WAF1} and tubulin acetylation expression levels. Methyl sulfide **15c** increased weakly these levels in line with its noticeable effect on the induction of differentiation. While the **11a–g** series did not show a significant effect on tubulin acetylation, some members (**11b–e**) up-regulated p21^{WAF1} to levels even higher than those of SAHA. The effect of the analogues on the level of histone acetylation was also analyzed by Western blot (Fig. 3D). After treating U937 cells for 24 h all compounds of the series **11a–g** displayed the ability to increase the level of acetylated histone H3, present in the histonic extract, as shown using the specific antibody.

In order to determine if the most potent analogues are endowed with additional epigenetic modulation activities, the series **11a–g** and **20** were also used in in vitro human SIRT1 fluorescent assay and in a radioactive assay on a peptide fragment having p300/CBP histone acetyl transferase (HAT) enzyme activity. As shown in Figure 4B, very weak SIRT1 inhibition was noted (ca. 30% relative to the control) for the majority of compounds at 50 μ M, far lower than the activity of the SIRT1 inhibitor suramin at the same concentration. In addition, none of the analogues displayed modulation of a peptide fragment of CBP containing the enzymatically active HAT domain (Fig. 4A) relative to the control and to the effects of the known inhibitor anacardic acid (AA) at the same concentration,^{65,66} thus confirming the specificity of the HDAC among other epigenetic inhibitory activities.

DNMT inhibition has also been reported for PsA.³ To verify the effective physical interaction between PsA and its analogues and DNA methyl transferase enzymes, two in vitro radioactive assays were performed using DNMT1 and DNMT3A (Fig. 4C and D). DNMT1 was immunoprecipitated from K562 cells and used in radioactive assay that employs [³H]-adenosyl-L-methionine as methyl donor and Poly dI-dC as methyl acceptor. The same conditions have been used for the DNMT3A radioactive assay, but the

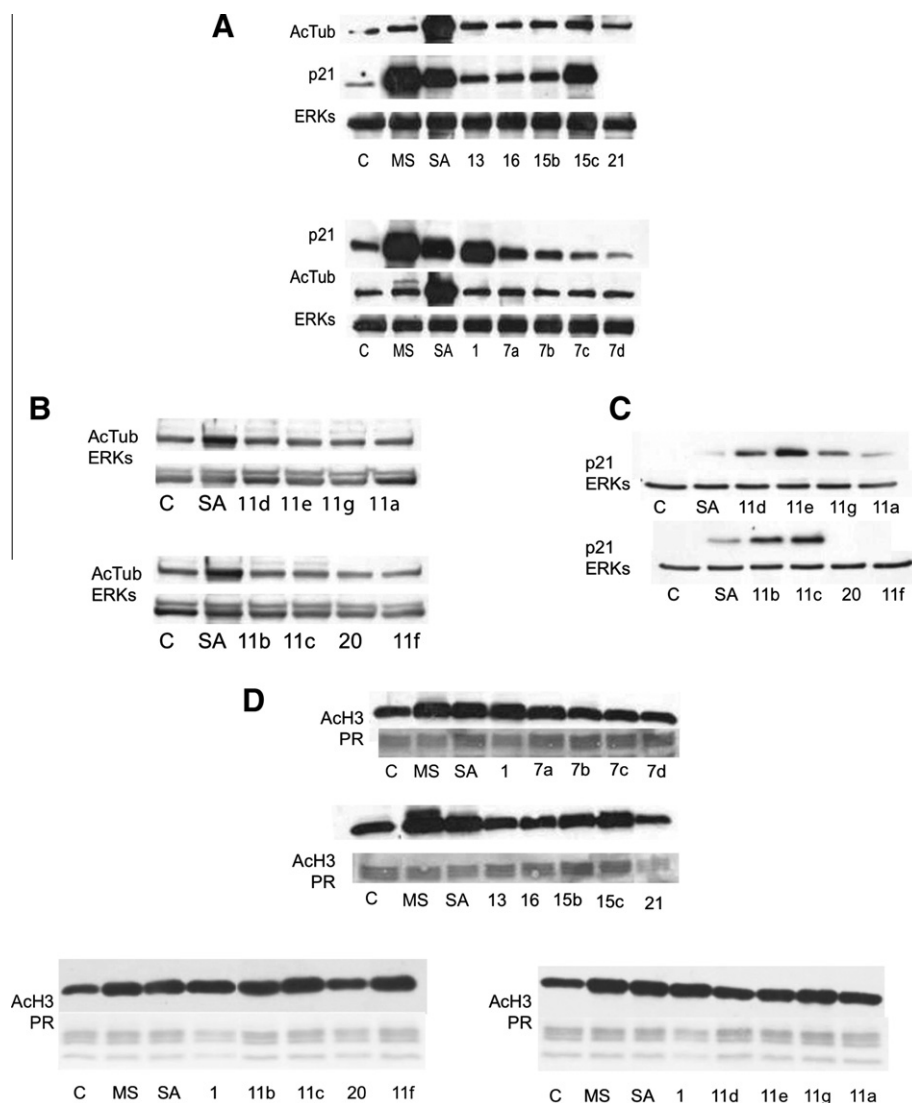


Figure 3. (A–C) Western blot analyses of p21^{WAF1/CIP1} expression and α -tubulin acetylation in U937 cells after treatment with the indicated compounds at 5 μ M for 24 h. ERK1 expression is shown as loading control. (D) Western blot analyses of histone H3 acetylation carried out in U937 cells, after 24 h induction with the compounds at 5 μ M.

recombinant enzyme was produced in *Escherichia coli* BL21, as GST fused protein. In neither assay compounds **11a–g** and **20** showed significant inhibition at 50 μ M (see Fig. 4C), in contrast to RG108⁶⁷ and SGI1027⁶⁸ at the same concentration for the DNMT1 assay.

Taken together, the enzymatic profiling suggests that the epigenetic activities of PsA are mainly restricted to the inhibition of the HDAC family in this context. Moreover, the HDAC activity of the series is likely linked to the formation of the monomeric thiol that originates from $-S \cdots S-$ bond cleavage (Scheme 7, vide infra), a known potent metal chelator. The Zn²⁺-dependent histone deacetylase subfamily is composed of Class I HDACs (HDAC 1–3, 8 and 11) and Class II HDACs (HDAC 4–7, 9 and 10). In contrast, Class III (sirtuins), with seven members (SIRT1–7), require NAD⁺ as a cofactor and release *O*-acetyl-ADP ribose and nicotinamide as a consequence of acetyl transfer from the acetylated lysine.⁶⁹

Metalloproteinase-targeted HDAC inhibitors are typically substrate mimics of the linear acetyl-lysine side chain with a Zn²⁺-chelating 'warhead' group that replaces the scissile acetamide, a connector chain and a 'cap' at the other end that extend beyond the enzyme substrate-binding channel. These features are exhibited by the thiol derived from PsA (Scheme 7), in which

the active site binding/inactivating group is connected via a hydroxyimino amide linker to the HDAC recognition aryl group.

In order to address the nature of the interaction between the inhibitor and HDAC, the ab initio calculated structure of thiol **22** was docked into the active site of the human HDAC8-trichostatin A (TSA) crystal structure⁷⁰ after removal of the TSA ligand. The catalytic domain of about 390 amino acids responsible for the deacetylation is highly conserved among the metal-dependent HDACs, in particular the residues lining the ligand-binding pocket, but some differences can be exploited for the designed of selective Class I/Class II HDAC inhibitors.⁷¹

The highest scores using automated docking method for the interaction of the ligand with the Zn²⁺ ion in the active site, validated by the GRID maps, agree in having the thiol chelated to the metal, whereas the linker domain occupies the channel and the *o*-bromophenol is stabilized through interaction with Tyr100 and Phe152 at the rim of the active site entrance (Fig. 5 and Figs. S1–S3). This positioning facilitates the formation of a hydrogen bond between the oxime group and Asp101, which remains at a constant distance along the energy minimization and the simulation of the dynamic behaviour using unrestrained MD (Fig. S3). The Zn²⁺ ion is kept firmly coordinated to the four ligands (Asp178, Asp267, His180 and the thiol group of the inhibitor),

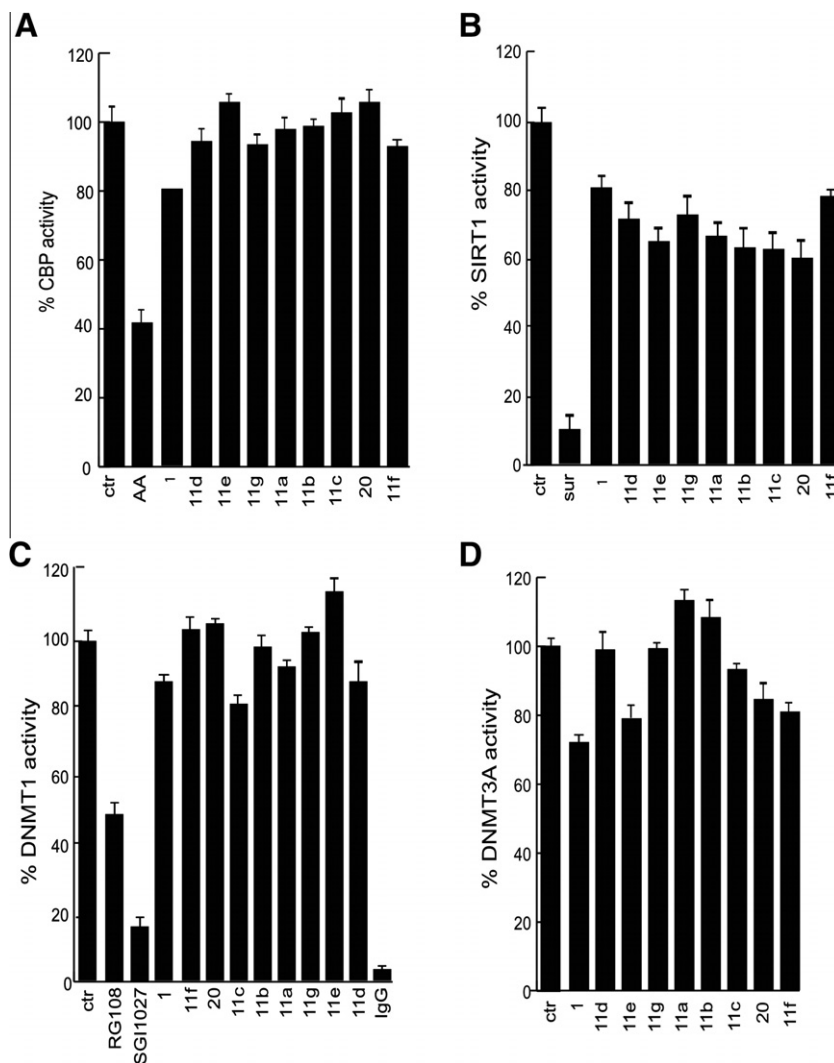
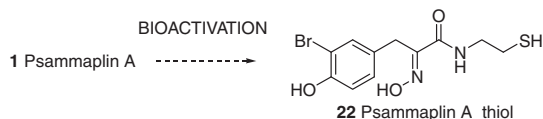


Figure 4. (A) CBP radioactive assay performed with 1 μ g of recombinant CBP enzyme peptide fragment and the psammaplin A analogues at 50 μ M. (B) SIRT1 fluorescence assay to measure the lysine deacetylase activity of the compounds at 50 μ M on human recombinant SIRT1 enzyme (1 U). (C) DNMT1 radioactive assay with synthetic poly dI-dC as methyl acceptor (0.1 μ g) and [3 H]-adenosyl-L-methionine (1 μ Ci) as methyl donor. DNMT1 was immunoprecipitated from K562 cells and the compounds **11a–g** were used at 50 μ M. (D) DNMT1 radioactive assay to measure the inhibition of recombinant DNMT3a (1 μ g, produced in *E. coli* BL21, as GST fused protein) by the compounds at 50 μ M. In each panel the inhibition/activation of the enzyme is reported as percentage of activity relative to the control.



Scheme 7. Bioactivation of PsA **1** to thiol **22** by the reductive environment of the cells.

and the electrostatic term (-59.2191 ± 1.7841 kcal/mol) makes an important contribution to the overall energy. Favourable van der Waals interactions of the ligand with Phe152 and Phe208 residues also account for a fraction of the intermolecular energy component (Fig. S2).

4. Discussion

Psammaplin A **1** is the prototype of a collection of metabolites isolated from sponges¹ that are biosynthesized by linear connections of (bromo)tyrosines and modified cysteines.¹² Their biological activities, common to most of the bromotyrosine/cysteine constructs, range from antimicrobial⁵⁴ to anticancer.^{1,6} The inhibi-

tion of several enzymes that impact different stages on the onset and progression of cancer such as topoisomerase II (growth),¹⁴ the zinc-dependent metalloproteinase aminopeptidase N (APN, tumor cell invasion or angiogenesis),²¹ HDAC and DNMT (chromatin remodeling),³ among others, likely conspire to account for the reported anticancer activities of PsA in several cancer cell lines and in the A549 lung xenograft mouse model.^{3,12} PsA was reported to activate Wnt signalling in a cell-based assay but the effect is likely due to HDAC inhibition rather than to an specific Wnt signalling pathway.⁷²

More recent molecular and cellular studies⁷³ confirmed the potent inhibitory activity of PsA in enzymatic (HDAC inhibition) and in anti-proliferation assays, and also the selective induction of histone hyperacetylation. The anti-proliferative effects were linked to the overexpression of genes related to cell cycle arrest and apoptosis (p53-independent p21^{WAF1} expression).⁷⁴

A series of PsA analogues modified at the aryl ring, with varying lengths of the amino thiol connecting unit, and some exchanges/deletions of functional groups have been prepared. These analogues have been characterized with regard to their enzymatic inhibitory potential and for their effects on cell cycle, differentia-

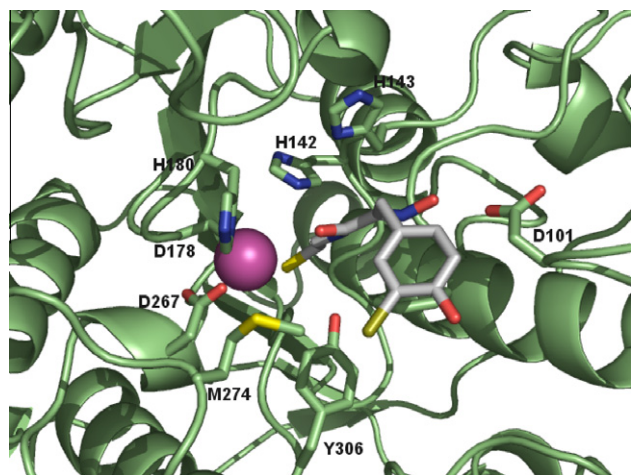


Figure 5. Proposed docking pose of biocleaved psammaplin A (thiol **22**) with HDAC8. The α trace of the enzyme is displayed as a ribbon, colored in green. The side chains of His142, His143, Asp178, Asp267, His180, Met274, Tyr306 are shown as sticks, with carbon atoms colored in green. The Zn^{2+} ion at the catalytic site is shown as a magenta sphere. The inhibitor is displayed also as sticks, but with carbon atoms colored in gray and the bromine atom colored in brown.

tion and apoptosis on the U937 acute myeloid leukemia cell line. For **1** and the most potent analogues, functional assays have also been carried out on the same cell line.

Enzymatic HDAC1 inhibition data for the series of analogues having chain lengths spanning from two to six methylene units (**7a–d**) established that the derivative of natural cystamine (the decarboxylated cysteine) present in psammaplin A was the most potent, and also that both the oxime and the disulfide functionalities were required for the HDAC inhibition activity, since analogues **13**, **15b–c**, **16** and **20** proved to be inactive (Fig. 1A). We then addressed the modifications of the aryl ring with analogues that preserve the same connecting diamine unit of the parent natural product. The substitution at the ring is well tolerated, and a general improvement in potency relative to PsA was noted when the ring was mono- (**11a–b**) or disubstituted (**11d,e,g**). The unsubstituted compound (the phenylalanine-derived **11c**) and the trisubstituted bromopsammaplin A **11f** were less active than **1**. Conversely the series of halogenated analogues **11d,e,g** exhibited greater potency than PsA and followed the order $\text{Br} < \text{F} < \text{Cl} < \text{I}$. The activities of the spiro derivative **21** are most intriguing, since it is the only compound showing a G2/M block (Fig. 1B) and strong induction of apoptosis (Fig. 2B), which appears not to be correlated with HDAC inhibition. A promising pro-differentiation profile is also noted for the methylsulfide **15c** (Fig. 2B), which merit further investigation.

It has previously been reported that human endometrial Ishikawa cancer cells treated with PsA showed accumulation of cells in the G1 phase and a significant decrease in the number of cells in the S phase,⁷⁴ a result in keeping with the effect of known HDAC inhibitors.⁷⁵ Our data confirm the time-dependent accumulation of cells in G1 upon treatment of human leukaemia U937 cells with PsA and analogues. Moreover, **1** and the **11a–g** series of related compounds induced apoptosis of U937 cells (Fig. 2B), an effect likely associated to their more selective inhibition of class I HDACs. The majority of these compounds (with the exception of **15c**) failed to induce tubulin acetylation (Fig. 3), which is a target of HDAC6 enzymes, and this finding is in agreement with previous reports for PsA in HeLa cells.⁷³ Although the result might suggest that psammaplin A show selectivity for histone proteins in preference to tubulin, it cannot be considered as a selective class I HDAC inhibitor, since it also inhibits HDAC4, a class II HDAC, in enzymatic assays (results not shown). Important differences between class I

and class II metallo-HDACs are noticeable in their size (with class II being from two to three times larger), their cellular localization, the conservation of sequence motifs in the catalytic domains, the identity of the protein–protein interaction complexes and the tissue distribution.⁷⁶

Western blot analysis of U937-treated cells confirmed the accumulation of acetylated histones using antibodies against acetylated H3 (Fig. 3D), in agreement with similar findings for PsA in endometrial cancer Ishikawa cells.⁷⁴ PsA and several analogues up-regulated cyclin-dependent kinase inhibitor p21^{WAF1} (Fig. 3), which is one of the genes induced by HDAC inhibitors,⁷⁶ and this effect might be related to the suppression of cell proliferation and induction of apoptosis.

PsA and its 5-bromo derivative have been reported to inhibit the bacterial methyltransferase SssI. However, cultured HCT116 human colon carcinoma cells treated with 1 μM PsA did not reduce global genomic DNA methylation (the level of which was determined using a mass spectrometry assay) and failed to induce the hypomethylation or reactivation of cancer-testis antigen genes, known as methylation silenced genes.⁵⁶ Here, two different assays were performed on DNMT1 and DNMT3A (see Fig. 4C and D) to evaluate the inhibition of DNMT enzymes by PsA and derivatives (**11a–g**). Differently from expected, these compounds at 50 μM failed to inhibit DNMT1 and DNMT3A, thus indicating their inability to alter DNMT in vitro. Therefore, the action of these compounds on cell cycle progression and induction of apoptosis can be better correlated with the HDAC inhibitory activities. It is likely that the absence of hypomethylation is not due to the low affinity of PsA (and its analogues) for DNMT, but instead to the inefficient transport of these compounds through the nuclear membrane. Inefficient transportation of the compound into the nucleus or poor cell membrane penetration might also explain the much greater concentration of **1** (1800 times) required to obtain similar potencies in cell-based assays relative to the HDAC enzymatic inhibition assay.⁵²

Lastly, no significant inhibition of SIRT1 and p300/CBP HAT enzymes was seen for the PsA-related series of analogues (Fig. 4A and B).

Other natural products of the depsipeptide class that act as inhibitors of HDAC also contain disulfide bonds, namely FK228 **23**, spiruchostatins **25** and FR901375 **26** (Fig. 6).^{39,71} FK228 (romi-

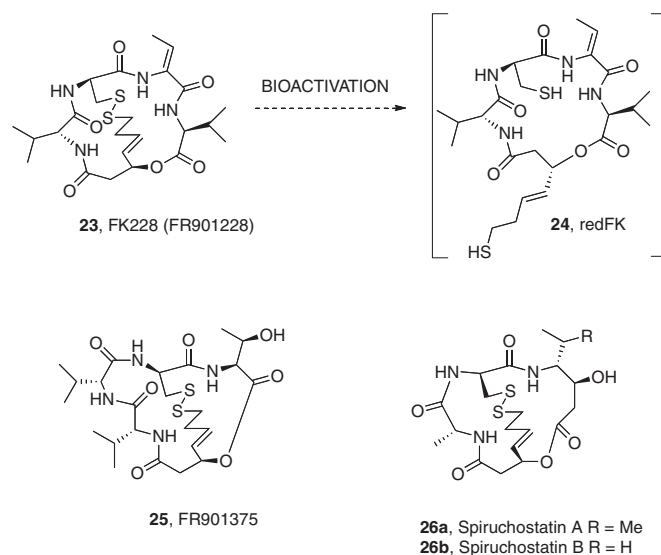


Figure 6. Natural depsipeptides **23–26** containing disulfide bonds are HDAC inhibitors. The structure of previously characterized active reduced form of FK228 (**24**, redFK) is shown by analogy with the reduced form of psammaplin A, **22**.

depsin, Istodax[®]) currently approved for T cell lymphoma is undergoing phase II clinical trials for the treatment of non-Hodgkin's lymphoma, acute myelogenous leukemia, and pancreatic cancer (www.clinicaltrials.gov). It has been shown that the disulfide bond of FK228 becomes cleaved in the cells by the reducing activity of glutathione to afford redFK **24**, and the thiol then interacts with the Zn²⁺ ion in the active site of HDAC.⁷⁷ Moreover, mass spectrometry analysis of blood samples identified the thiol and glutathione conjugates of FK228.⁷⁸ Upon bio-reduction depsipeptides **25** and **26** must also release the Zn²⁺-binding butenylthiol.⁷⁹ From an structural point of view both redFK **25** and PsA thiol **22** have Zn²⁺ ion connecting chains that are shorter than those of common hydroxamic acid-based inhibitors (TSA, SAHA. . .). Thiol chelating groups connected via a 5 atom saturated chain to cyclic tetrapeptides have also shown potent HDAC inhibitory activities.^{80,81}

In agreement with these precedents, the dimer analogue lacking the disulfide bond (**13**) was inactive, which substantiates the proposal that PsA and analogues undergo thiolate exchange reaction with glutathione by –S·S– bond cleavage.⁸² Interestingly, Wang et al. have shown that glutathione-depleted cells were not sensitive to PsA, implying that the reducing environment of the cells triggered the conversion of the disulfide of **1** to the corresponding thiol,⁷⁹ which would be the species responsible for the HDAC inhibitory activity of psammaplin A after uptake into the cells.

Based on the reported crystal structure, the HDAC8·Zn²⁺·thiol **22** complex was constructed with the thiol group chelating the metal ion, and then refined using energy minimization. The dynamic behaviour of the complex using unrestrained molecular dynamics confirmed the feasibility of the proposed binding orientation and the mutual adaptation between HDAC8 and the ligand. The linker occupies the narrow channel whereas the bromophenol interacts with Tyr100 and Phe152 at the rim of the active site entrance, a pose that facilitates the formation of a robust hydrogen bond between the oxime group and Asp101 (Fig. 5).

Our results using alcohol **16**, ether **15b** and most importantly dimer **13** confirm the earlier findings with FK228⁷⁸ and suggest that psammaplin A **1** acts as a stable pro-drug⁸³ that is activated upon uptake by the reductive environment of the cells to afford thiol **22**, which then chelates the Zn²⁺ ion in the active site of the HDAC metalloenzymes.

5. Conclusion

PsA **1**, a natural product with a disulfide bond derived from the condensation of modified cystamine and tyrosine moieties, has been reported to display dual HDAC and DNMT epigenetic inhibitory activities. The intriguing ability to target simultaneously more than one member of the epigenetic machinery (epigenetic multiple ligands),⁸⁴ prompted us to synthesize a series of PsA analogues in an effort to determine the structural determinants for their epigenetic profile. We have analyzed the effects of the natural-product inspired collection on the human leukaemia U937 cell cycle, measuring induction of apoptosis and differentiation, induction of p21^{WAF1} and tubulin acetylation levels and total histone H3, and also examined their HDAC1 enzyme-based inhibition profile. From the results it is concluded that Nature has optimized the design of the PsA scaffold to fulfil this epigenetic role, since only closely related synthetic derivatives (with modifications at the bromotyrosine ring) exhibited comparable or greater potency than the natural product. Modifications of the connecting chain, oxime bond and disulfide unit afforded either inactive or considerable less potent analogues. Exploring the possibility that PsA and derivatives might display additional epigenetic activities we have also tested them as inhibitors of DNMT1, DNMT3A, SIRT1 and a peptide containing the p300/CBP HAT domain, but the values measured were

very low. Since epigenetic signalling by PsA appears to be restricted to inhibition of metalloproteinase HDACs, a model for the interaction of HDAC8 with the thiol derived from PsA **1** (by a presumed *in vivo* disulfide cleavage) was computed. The thiol binds the Zn²⁺ ion in the active site and the complex is additionally stabilized by a hydrogen bond interaction between the oxime group and the Asp101 residue located at the active site entrance. As with FK228, this bioactivation mechanism illustrates the ingenious solution adopted by Nature to protect the reactive zinc-binding thiol as a disulfide pro-drug with higher bioavailability. The increased levels of disulfide reductants (i.e., glutathione, thioredoxin and thioredoxin reductase) found in many cancer cells render such cells particularly susceptible to the action of PsA **1**.

Despite the failure to greatly improve the epigenetic inhibitory profile of PsA through the modifications reported, more significant skeletal alterations of the PsA structure might provide more potent derivatives, thus lending further support to the important role of natural products as inspiration⁸⁵ for the development of designed multiple ligands^{50,51} as new anticancer drugs.^{86,87}

6. Experimental section

6.1. General

Solvents were dried according to published methods and distilled before use. HPLC grade solvents were used for the HPLC purification. All other reagents were commercial compounds of the highest purity available. All reactions were carried out under argon atmosphere, and those not involving aqueous reagents were carried out in oven-dried glassware. Analytical thin layer chromatography (TLC) was performed on aluminium plates with Merck Kieselgel 60F254 and visualized by UV irradiation (254 nm) or by staining with a solution of phosphomolibdic acid. Flash column chromatography was carried out using Merck Kieselgel 60 (230–400 mesh) under pressure. Infrared spectra were obtained on JASCO FTIR 4200 spectrophotometer, from a thin film deposited onto a NaCl glass. ¹H NMR spectra were recorded in CDCl₃, CD₃OD, DMSO-*d*₆ and (CD₃)₂CO at ambient temperature on a Bruker AMX-400 spectrometer at 400 MHz with residual protic solvent as the internal reference (CDCl₃, δ_H = 7.26 ppm; (CD₃)₂CO, δ_H = 2.05 ppm; CD₃OD, δ_H = 3.31 ppm; DMSO-*d*₆, δ_H = 2.50 ppm); chemical shifts (δ) are given in parts per million (ppm), and coupling constants (*J*) are given in Hertz (Hz). The proton spectra are reported as follows: δ (multiplicity, coupling constant *J*, number of protons, assignment). ¹³C NMR spectra were recorded in CDCl₃, CD₃OD, DMSO-*d*₆ and (CD₃)₂CO at ambient temperature on the same spectrometer at 100 MHz, with the central peak of CDCl₃ (δ_C = 77.0 ppm), CD₃OD (δ_C = 49.0 ppm), DMSO-*d*₆ (δ_C = 39.4 ppm) or (CD₃)₂CO (δ_C = 30.8 ppm) as the internal reference. The DEPT135 sequence was used to aid in the assignment of signals on the ¹³C NMR spectra. Melting points were determined on a Stuart SMP10 apparatus. Elemental analyses were determined on a Carlo Erba EA 1108 analyzer. MS experiments were performed on an APEX III FT-ICR MS (Bruker Daltonics, Billerica, MA), equipped with a 7T actively shielded magnet. Ions were generated using an Apollo API electrospray ionization (ESI) source (Bruker Daltonics, Billerica, MA), with a voltage between 1800 and 2200 V (to optimize ionisation efficiency) applied to the needle, and a counter voltage of 450 V applied to the capillary. Samples were prepared by adding a spray solution of 70:29.9:0.1 (v/v/v) methanol/water/formic acid to a solution of the sample at a v/v ratio of 1–5% to give the best signal-to-noise ratio. Data acquisition and data processing were performed using the XMASS software, version 6.1.2 (Bruker Daltonics). FAB experiments were performed on a VG AutoSpec instrument, using 3-nitrobenzylalcohol or glycerol as matrix.

6.2. General procedure for the oxidation of amines with Na₂WO₄

To a solution of amine (18.0 mmol) in EtOH (40 mL) at 0 °C were added Na₂WO₄·2H₂O (18 mmol), 30% H₂O₂ (16 mL) and H₂O (30 mL). The resulting mixture was stirred for 4 h at room temperature and the reaction was quenched with aqueous saturated NH₄Cl and extracted with EtOAc (3×). The combined organic extracts were washed with brine, dried over Na₂SO₄ and evaporated. The residue was purified by column chromatography on silica gel as indicated.

6.3. General procedure for the hydrolysis of esters

Lithium hydroxide (15 mmol) was added to a solution of ester (1 mmol) in a 1:1 THF/H₂O (16 mL) mixture. The solution was stirred at room temperature for 2 h, neutralized with 10% HCl and extracted with EtOAc (4×). The combined organic layers were washed with brine, dried over Na₂SO₄, filtered and the solvent was evaporated in vacuo. Crystallization of the residue provided the desired acid as indicated.

6.4. General procedure for the amidation of tyrosine acid derivatives with amines

N-Hydroxyphthalimide (1 mmol) and DCC (1 mmol) were added to a solution of the carboxylic acid (1 mmol) in dioxane (2.5 mL). After the mixture had been stirred for 2 h at room temperature, a solution of the amine (0.5 mmol), Et₃N (2 mmol) and MeOH (1 mL) was added. The resulting mixture was stirred for 12 h at room temperature and the reaction was quenched with H₂O and extracted with EtOAc (3×). The combined organic extracts were washed with brine, dried over Na₂SO₄ and evaporated. The residue was dissolved in THF, filtered off and the solvent was evaporated in vacuo. The resulting residue was then purified by column chromatography on silica gel as indicated.

6.4.1. (*E*)-Methyl 2-(hydroxyimino)-3-(4-hydroxyphenyl)propanoate (**3**)⁸⁸

Following the general procedure for the oxidation of amines with Na₂WO₄·2H₂O, *L*-tyrosine methyl ester **2** (3.45 g, 17.68 mmol) gave, after purification by column chromatography (SiO₂, 50:50 hexane/EtOAc), 2.24 g (60%) of oxime **3** as a white powder. ¹H NMR (CD₃COCD₃, 400.13 MHz): δ 11.35 (s, 1H, OH), 8.11 (s, 1H, OH), 7.11 (d, *J* = 8.5 Hz, 2H, ArH), 6.73 (d, *J* = 8.5 Hz, 2H, ArH), 3.84 (s, 2H, 2H₃), 3.72 (s, 3H, CO₂CH₃) ppm.

6.4.2. (*E*)-Methyl 3-(3-bromo-4-hydroxyphenyl)-2-(hydroxyimino)propanoate (**4**)⁶¹

A solution of NBS (0.49 g, 2.75 mmol) in CH₃CN (6 mL) was added dropwise over 15 min to the solution of the oxime **3** (0.58 g, 2.75 mmol) in CH₃CN (6 mL). The reaction mixture was stirred at room temperature for 5 h, after which time the solvent was evaporated and the residue was treated with water and extracted with EtOAc (3×). The combined organic extracts were dried over Na₂SO₄, filtered, evaporated and the residue was purified by column chromatography (SiO₂, 50:50 hexane/EtOAc) to afford oxime **4** (0.65 g, 82%) as a yellow powder. ¹H NMR (CD₃COCD₃, 400.13 MHz): δ 11.49 (s, 1H, OH), 8.62 (s, 1H, OH), 7.44 (d, *J* = 1.6 Hz, 1H, H_{2'}), 7.13 (dd, *J* = 8.3, 1.6 Hz, 1H, H_{6'}), 6.90 (d, *J* = 8.3 Hz, 1H, H_{5'}), 3.85 (s, 2H, 2H₃), 3.74 (s, 3H, CO₂CH₃) ppm.

6.4.3. (*E*)-3-(3-Bromo-4-hydroxyphenyl)-2-(hydroxyimino)propanoic Acid (**5**)

In accordance with the general procedure for the hydrolysis of esters, ester **4** (0.61 g, 2.11 mmol) gave, after purification by column chromatography (SiO₂, 90:10 EtOAc/MeOH), 0.58 g (99%) of

acid **5** as a white powder, mp: 147–148 °C (hexane/CHCl₃) (lit. 147–148 °C, dec.).⁸⁹ ¹H NMR (CD₃COCD₃, 400.13 MHz): δ 7.45 (s, 1H, H_{2'}), 7.14 (d, *J* = 7.9 Hz, 1H, ArH), 6.90 (d, *J* = 7.9 Hz, 1H, ArH), 3.84 (s, 2H, 2H₃) ppm.

6.4.4. (2*E*,2'*E*)-*N,N'*-[2,2'-Disulfanediy]bis(ethane-2,1-diyl)]bis[3-(3-bromo-4-hydroxyphenyl)-2-(hydroxyimino)propanamide] (psammaplin A, **1**)⁵⁶

Following the general procedure for the amidation of tyrosine acid derivatives with amines, acid **5** (0.16 g, 0.59 mmol) afforded, after purification by column chromatography (SiO₂, gradient from 25:75 hexane/EtOAc to 95:5 CH₂Cl₂/MeOH), psammaplin A **1** (0.12 g, 60%) as a white foam. ¹H NMR (CD₃OD, 400.13 MHz) (data for monomer): δ 7.36 (s, 1H, H_{2'}), 7.07 (d, *J* = 8.3 Hz, 1H, ArH), 6.76 (d, *J* = 8.3 Hz, 1H, ArH), 3.79 (s, 2H, 2H₃), 3.52 (t, *J* = 6.7 Hz, 2H, 2H_{1''}), 2.81 (t, *J* = 6.7 Hz, 2H, 2H_{2''}), 2.15 (br, 2H, OH) ppm.

6.5. Molecular modeling of psammaplin A

6.5.1. Quantum mechanics calculations

The geometry of the thiol derived from psammaplin A was optimized using the ab initio quantum chemistry program Gaussian 03⁹⁰ and the HF/3-21G* basis set. A set of atom-centred RHF 6-31G**/3-21G* charges was then obtained by using the RESP methodology⁹¹ as implemented in the AMBER suite of programs (<http://amber.scripps.edu/>). Covalent and nonbonded parameters for the inhibitor atoms were assigned, by analogy or through interpolation, from those already present in the AMBER force field⁹² (parm99) or consistently derived, as explained in more detail elsewhere.⁹³

6.5.2. Molecular docking

The genetic algorithm⁹⁴ implemented in AutoDock⁹⁵ and the h-HDAC8 (PDB code 1t64)⁷⁰ as the target protein upon removal of trichostatin A was used to generate different HDAC-Zn²⁺-bound psammaplin A thiol conformers by randomly changing torsion angles and overall orientation of the molecule. A volume for exploration was defined in the shape of a three-dimensional cubic grid with a spacing of 0.3 Å that enclosed the residues that are known to make up the inhibitors binding pocket. At each grid point, the receptor's atomic affinity potentials for carbon, oxygen, nitrogen, sulfur, bromine and hydrogen atoms present in the ligand were precalculated for rapid intra- and intermolecular energy evaluation of the docking solution.

To obtain additional validation of the proposed binding mode for the ligands, the program GRID (<http://www.moldiscovery.com/>)⁹⁶ was also used to search for sites on the enzyme that could be complementary to the functional groups present in this inhibitor. For the GRID calculations, a 18 × 21 × 21 Å lattice of points spaced at 0.5 Å was established at the binding site. The probes used were C1 = (aromatic carbon), N1 (neutral flat NH, eg amide), N:# (sp nitrogen with lone pair), O (sp² carbonyl oxygen) and Br (bromine). The dielectric constants chosen were 4.0 for the macromolecule and 80.0 for the bulk water.

6.5.3. Molecular dynamics simulations

Ternary complexes (HDAC8-Zn²⁺-psammaplin A thiol) representative of the most populated solutions were then refined using the second generation AMBER force field and 3000 steps of steepest descent energy minimization and 6000 steps of conjugate gradient of only the side chain of the protein and those atoms of the bound ligand. This procedure allowed readjustment of covalent bonds and van der Waals contacts without changing the overall conformation of the complex. The HDAC-psammaplin A thiol complex was then neutralized by addition of eight sodium ions⁹⁷ that were placed in electrostatically favored positions and immersed

in rectangular boxes each containing about 450 TIP3P water molecules⁹⁸ that extended 1 Å away from any solute atom. The cutoff distance for the non-bonded interactions was 9 Å, and periodic boundary conditions were applied. Electrostatic interactions were represented using the smooth particle mesh Ewald method with a grid spacing of ~1 Å. Unrestrained molecular dynamics (MD) simulations at 300 K and 1 atm were then run for 6 ns using the SANDER module in AMBER 8.⁹⁹ The coupling constants for the temperature and pressure baths were 1.0 and 0.2 ps, respectively. SHAKE¹⁰⁰ was applied to all bonds involving hydrogens, and an integration step of 2 fs was used throughout. The nonbonded pair list was updated every 10 steps. The simulation protocol involving a series of progressive energy minimizations followed by a 20 ps heating phase and a 70 ps equilibration period before data collection. System coordinates were saved every 2 ps for further analysis.

6.5.4. Analysis of the molecular dynamics trajectories

Three-dimensional structures and trajectories were visually inspected using the computer graphics program InsightII. The root-mean-square (rms) deviations from both the initial structures and the average structures, the inter-atomic distances, and the snapshot geometries were obtained using the PTRAJ module in AMBER. Intermolecular van der Waals energies for individual residues were calculated with the ANAL module, whereas the solvent-corrected residue-based electrostatic interaction energies were calculated with DelPhi, following the procedure described.⁹³

All calculations were performed on the SGI R14000 Origin 3800 at CIEMAT (Madrid), on the SGI 1.5 GHz Itanium2 at CESGA (Santiago de Compostela) and locally on SGI R12000 Octane workstations.

6.6. Biological assays

6.6.1. Cell culture

Human leukaemia cell lines U937, K562 and HL60 were propagated in RPMI medium supplemented with 10% FBS (Foetal bovine serum; Hyclone) and antibiotics (100 U/mL penicillin, 100 µg/mL streptomycin and 250 ng/mL amphotericin-B). Cells were kept at the constant concentration of 200,000 cells per mL of culture medium.

6.6.2. Ligands and materials

SAHA (Merck) and MS-275 (a kind gift of Bayer-Schering AG) were dissolved in DMSO and used at 5×10^{-6} M. All other compounds described were dissolved in DMSO (Sigma-Aldrich) and used at 5 and 50 µM.

6.6.3. Cell cycle analysis

2.5×10^5 cells were collected and resuspended in 500 µL of hypotonic buffer (0.1% Triton X-100, 0.1% sodium citrate, 50 µg/mL propidium iodide, RNase A). Cells were incubated in the dark for 30 min. Samples were acquired on a FACS-Calibur flow cytometer using the Cell Quest software (Becton Dickinson) and analysed with standard procedures using the Cell Quest software (Becton Dickinson) and the ModFit LT version 3 Software (Verity) as previously reported.^{101,102} Apoptosis was revealed by monitoring nuclear fragmentation (the so-called 'sub-G1 DNA peak') by FACS and analysed by Cell Quest technology.

6.7. Caspase 3 activation assay

Caspase activity was detected in living U937 cells using the BIOMOL and B-BRIDGE Kits supplied with cell-permeable fluorescent substrates. The fluorescent substrate for caspase 3 was FAM-DEVD-FMK, ca. 1×10^6 cells were washed twice in cold PBS and incubated for 1 h in ice with the corresponding substrates as rec-

ommended by the suppliers. The cells were analysed after washing using the CellQuest software applied to a FACScalibur (BD). Experiments were performed in duplicate and values were expressed as mean ± SD.

6.7.1. Granulocyte differentiation

Granulocyte differentiation was carried out as previously described.¹⁰³ Briefly, U937 cells were harvested and resuspended in 10 µL phycoerythrin-conjugated CD11c (CD11c-PE). Control samples were incubated with 10 µL PE conjugated mouse IgG1 for 30 min at 4 °C in the dark, washed in PBS and resuspended in 500 µL PBS containing propidium iodide (0.25 µg/mL). Samples were analyzed by FACS with Cell Quest technology (Becton Dickinson). Propidium iodide (PI) positive cells have been excluded from the analysis.

6.7.2. Western blot analyses

Western blot analyses were performed according to standard procedures following suggestions of antibody suppliers. For the determination of p21^{WAF1/CIP1} 50 µg of total protein extracts were separated on a 15% polyacrylamide gels and blotted. Western blots were shown for p21 (Transduction Laboratories, dilution 1:500) and total ERKs (Santa Cruz) were used to normalize for equal loading. For α -Tubulin acetylation 25 µg of total protein extracts were separated on a 10% polyacrylamide gels and blotted. Western blots were shown for acetylated α -tubulin (Sigma, dilution 1:500) and total ERKs (Santa Cruz) or total tubulin (Sigma) were used to normalise for equal loading.

6.8. Histone extraction protocol

Cells were harvested and washed twice with ice-cold PBS and lysed in Triton Extraction Buffer (TEB: PBS containing 0.5% Triton X 100 (v/v), 2 mM phenyl methyl sulfonyl fluoride (PMSF), 0.02% (w/v) NaN₃) at a cellular density of 10^7 cells per mL for 10 min on ice, with gentle stirring. After a brief centrifugation at 2000 rpm at 4 °C, the supernatant was removed and the pellet was washed in half the volume of TEB and centrifuged as before. The pellet was resuspended in 0.2 M HCl at a cell density of 4×10^7 cells per mL and acid extraction was left to proceed overnight at 4 °C on a rolling table. Next, the samples were centrifuged at 2000 rpm for 10 min at 4 °C, the supernatant was removed and protein content was determined using the Bradford assay.

6.9. Determination of histone H3 specific acetylations

For the histone H3 acetylation in U937 cells, 10 µg of histone extract was separated on 15% polyacrylamide gels and blotted. Western blots were shown for pan-acetylated histone H3 (Upstate).

6.10. Fluorimetric human recombinant HDAC1 assays

GST-HDAC1 has been cloned into the pAcG2T baculovirus transfer vector (BD) and purified by using glutathione beads. The BD BaculoGold transfection system (BD) has been used in Sf9 insect cells for expression following supplier's instructions. The HDAC assay has been carried out as follows: the HDAC Fluorescent Activity Assay is based on the Fluor de Lys Substrate and Developer combination (BioMol) and has been carried out according to supplier's instructions. Briefly, the Fluor de Lys Substrate, which comprises an acetylated lysine side chain, has been incubated with the purified recombinant HDAC enzymes in presence or absence of the inhibitors, for 0.5 h at 37 °C. When a different incubation time has been used, it is specified into the text. Deacetylation of the substrate sensitizes the substrate so that, in the second step, treatment

with the Developer for 30 min produces a fluorophore. The fluorophore is excited with a 360 nm light and the emitted light (460 nm) has been quantified with a TECAN Inphinite M200 station.

6.11. Human recombinant Sirt1 assay

Recombinant human Sirt1 was prepared in *E. coli* BL21 and purified by affinity chromatography. The enzymatic reaction consisted of 1 µg of Sirt1 incubated with the acetylated p53 peptide (AA 379–382), 1 mM dithiothreitol, and a range of inhibitor concentrations, as described. Reactions were carried out at 37 °C for 60 min. Assays were performed in the presence of 200 µM NAD⁺ for each inhibitor. Fluorescence was measured with a fluorimetric reader (TECAN Inphinite M200 fluorescence plate reader) with excitation set at 360 nm and emission detection set at 450 nm. Results are expressed as the mean and standard deviation of four independent experiments as percentage of activity considering the untreated control as 100.

6.12. Human recombinant CBP assay

The recombinant CBP was prepared in *E. coli* BL21 and purified by affinity chromatography. Recombinant CBP fraction corresponded to amino acids 1098–1877. CBP was incubated in HAT buffer with 10 µg of histone H4 peptide (corresponding to amino acids 2–24) and 20 µM Acetyl CoA containing 0.5 µCi/mL [³H]-Acetyl CoA in the presence of inhibitors. After 2 h at 37 °C, 5 µL of samples were spotted onto Whatman P81 paper (in triplicate). The paper squares were washed three times in 5% TCA and once in 100% acetone and then placed into scintillation vials containing scintillation fluid to allow the DPM reading. The DPM of enzyme samples was compared to DPM of negative control. Data have been expressed as percentage of activity considering the control without treatment as 100.

6.13. Human recombinant DNMT3A radioactive assay

DNMT3A was produced in *E. coli* BL21 according to standard procedures. The methyltransferase radioactive assay was performed in a volume of 25 µL/point, using [³H]-adenosyl-L-methionine (1 µCi) as methyl donor and Poly dI-dC (0.1 γ) as methyl acceptor, while 30–50 ng of recombinant DNMT3A protein was used, depending on enzyme activity, stability and purity. The compounds were tested at 50 µM. After 2 h incubation at 37 °C, 5 µL of samples were spotted onto Whatman DE81 paper (in triplicate). The paper squares were washed three times in 5% Na₂HPO₄ and once in sterile water and then placed into scintillation vials containing 5 mL of scintillation fluid to allow the DPM reading. The DPM of enzyme samples was compared to the DPM of negative control. Data were expressed as a percentage of activity relative to control.

6.14. Immunoprecipitation of DNMT1 and radioactive assay

The K562 cells were cultured in the experimental conditions reported and lysed in TAP buffer pH 7–7.5 (50 mM Tris pH 7.0, 180 mM NaCl, 0.15% v/v NP40, 10% v/v glycerol, 1.5 mM MgCl₂, 1 mM Na₂MoO₄, 0.5 mM NaF, 1 mM DTT, 0.2 mM PMSF, 0.1 mM protease inhibitor cocktail) for 10 min in ice and centrifuged at 130,000 rpm for 30 min. 650 µg of extracts were diluted in TAP buffer up to 1 mL and pre-cleared by incubating with 20 µL A/G plus agarose (Santa Cruz) for 30 min to 1 h on a rocking table at 4 °C. Supernatant was transferred to a new tube and 3–5 µg of antibody against DNMT1 (Abcam) was added. IP was allowed to proceed overnight at 4 °C on a rocking table. As a negative control

the same amount of protein extracts were immunoprecipitated with purified IgG rabbit (Santa Cruz). The following day, 50 µL A/G plus agarose was added and incubation was continued for 2 h. The beads were recovered by brief centrifugation and washed with cold TAP buffer several times. After the last washing 20 µL of 2X concentrated electrophoresis sample buffer (217 mM Tris–HCl pH 8.0, 5.3% SDS, 17.4% glycerol, 8.7% β-mercaptoethanol, 0.026% bromophenol blue) was added and the sample was boiled for 5 min. A fraction of supernatants was loaded onto an SDS–PAGE gel in order to check the immunoprecipitation product. 10 µL of resin binding DNMT1 were used in DNMT radioactive assay (see above) to test the inhibitory potency of the PsA derivatives.

Acknowledgments

This work was supported by the EU (Epi tron LSHC-CT2005-518417; JG, RP, GLF and AN contracts; and ATLAS Contract 221952), the Spanish MICINN (SAF-07-63880-FEDER), Xunta de Galicia (INBIOMED), and the Italian Associazione Italiana per la ricerca contro il cancro.

Supplementary data

Supplementary data associated with this article can be found, in the online version, at doi:10.1016/j.bmc.2010.12.026.

References and notes

- Peng, J.; Li, J.; Hamann, M. T. *Alkaloids: Chem. Biol.* **2005**, *61*, 59.
- Jiménez, C.; Crews, P. *Tetrahedron* **1991**, *47*, 2097.
- Piña, I. C.; Gautschi, J. T.; Wang, G. Y. S.; Sanders, M. L.; Schmitz, F. J.; France, D.; Cornell-Kennon, S.; Sambucetti, L. C.; Remiszewski, S. W.; Perez, L. B.; Bair, K. W.; Crews, P. *J. Org. Chem.* **2003**, *68*, 3866.
- Arabshahi, L.; Schmitz, F. J. *J. Org. Chem.* **1987**, *52*, 3584.
- Rodríguez, A. D.; Akee, R. K.; Scheuer, P. J. *Tetrahedron Lett.* **1987**, *28*, 4989.
- Quiñoa, E.; Crews, P. *Tetrahedron Lett.* **1987**, *28*, 3229.
- Suzuki, A.; Matsunaga, K.; Shin, H.; Tabudrav, J.; Shizuri, Y.; Ohizumi, Y. *J. Pharmacol. Exp. Ther.* **2000**, *292*, 725.
- Shin, J.; Lee, H. S.; Seo, Y.; Rho, J. R.; Cho, K. W.; Paul, V. J. *Tetrahedron* **2000**, *56*, 9071.
- Pham, N. B.; Butler, M. S.; Quinn, R. J. *J. Nat. Prod.* **2000**, *63*, 393.
- Tabudravu, J. N.; Eijsink, V. G. H.; Gooday, G. W.; Jaspars, M.; Komander, D.; Legg, M.; Synstad, B.; Van Aalten, D. M. F. *Bioorg. Med. Chem.* **2002**, *10*, 1123.
- Jung, J. H.; Sim, C. J.; Lee, C.-O. *J. Nat. Prod.* **1995**, *58*, 1722.
- Park, Y.; Liu, Y.; Hong, J.; Lee, C. O.; Cho, H.; Kim, D. K.; Im, K. S.; Jung, J. H. *J. Nat. Prod.* **2003**, *66*, 1495.
- Kim, D.; Lee, I. S.; Jung, J. H.; Yang, S. I. *Arch. Pharm. Res.* **1999**, *22*, 25.
- Kim, D.; Lee, I. S.; Jung, J. H.; Lee, C. O.; Choi, S. U. *Anticancer Res.* **1999**, *19*, 4085.
- Nicholas, G. M.; Eckman, L. L.; Ray, S.; Hughes, R. O.; Pfefferkorn, J. A.; Barluenga, S.; Nicolaou, K. C.; Bewley, C. A. *Bioorg. Med. Chem. Lett.* **2002**, *12*, 2487.
- Jiang, Y.; Ahn, E. Y.; Ryu, S. H.; Kim, D. K.; Park, J. S.; Yoon, H. J.; You, S.; Lee, B. J.; Lee, D. S.; Jung, J. H. *BMC Cancer* **2004**, *4*, 70.
- Fajas, L.; Egler, V.; Reiter, R.; Hansen, J.; Kristiansen, K.; Debril, M.-B.; Miard, S.; Auwerx, J. *Dev. Cell* **2002**, *3*, 903.
- Fajas, L.; Egler, V.; Reiter, R.; Miard, S.; Lefebvre, A.-M.; Auwerx, J. *Oncogene* **2003**, *22*, 4186.
- Fu, M.; Rao, M.; Bouras, T.; Wang, C.; Wu, K.; Zhang, X.; Li, Z.; Yao, T.-P.; Pestell, R. G. *J. Biol. Chem.* **2005**, *280*, 16934.
- Mora, F. D.; Jones, D. K.; Desai, P. V.; Patny, A.; Avery, M. A.; Feller, D. R.; Smillie, T.; Zhou, Y. D.; Nagle, D. G. *J. Nat. Prod.* **2006**, *69*, 547.
- Shim, J. S.; Lee, H.-S.; Shin, J.; Kwon, H. J. *Cancer Lett.* **2004**, *203*, 163.
- Allis, C. D.; Jenuwein, T.; Reinberg, D.; Caparros, M.-L. *Epigenetics*; Cold Spring Harbor Laboratory Press: Cold Spring Harbor (NY), 2007.
- Sippl, W.; Jung, M. In *Epigenetic Targets in Drug Discovery: Methods and Principles of Medicinal Chemistry*; Mannhold, R., Kubinyi, H., Folkers, G., Eds.; Wiley: Weinheim, 2009; Vol. 42.
- Archer, S. Y.; Hodin, R. A. *Curr. Opin. Gene Dev.* **1999**, *9*, 171.
- Marks, P. A.; Rifkind, R. A.; Richon, V. M.; Breslow, R.; Miller, T.; Kelly, W. K. *Nat. Rev. Cancer* **2001**, *1*, 194.
- Rosato, R. R.; Grant, S. *Cancer Biol. Ther.* **2003**, *2*, 30.
- Blanchard, F.; Chipoy, C. *Drug Discovery Today* **2005**, *10*, 197.
- Bolden, J. E.; Peart, M. J.; Johnstone, R. W. *Nat. Rev. Drug Disc.* **2006**, *5*, 769.
- Lin, H. Y.; Chen, C. S.; Lin, S. P.; Weng, J. R.; Chen, C. S. *Med. Res. Rev.* **2006**, *26*, 397.
- Mei, S.; Ho, A. D.; Mahlknecht, U. *Int. J. Oncol.* **2004**, *25*, 1509.

31. Minucci, S.; Pelicci, P. G. *Nat. Rev. Cancer* **2006**, *6*, 38.
32. Fouladi, M. *Cancer Invest.* **2006**, *24*, 521.
33. Botrugno, O. A.; Santoro, F.; Minucci, S. *Cancer Lett.* **2009**, *280*, 134.
34. Mai, A.; Altucci, L. *Int. J. Biochem. Cell Biol.* **2009**, *41*, 199.
35. Kazantsev, A. G.; Thompson, L. M. *Nat. Rev. Drug Disc.* **2008**, *7*, 854.
36. Marks, P. A.; Dokmanovic, M. *Expert Opin. Invest. Drugs* **2005**, *14*, 1497.
37. Drummond, D. C.; Noble, C. O.; Kirpotin, D. B.; Guo, Z.; Scott, G. K.; Benz, C. C. *Ann. Rev. Pharmacol. Toxicol.* **2005**, *45*, 495.
38. Rodriguez, M.; Aquino, M.; Bruno, I.; De Martino, G.; Taddei, M.; Gomez-Paloma, L. *Curr. Med. Chem.* **2006**, *13*, 1119.
39. Paris, M.; Porcelloni, M.; Binaschi, M.; Fattori, D. *J. Med. Chem.* **2008**, *51*, 1505.
40. Smith, K. T.; Workman, J. L. *Int. J. Biochem. Cell Biol.* **2009**, *41*, 21.
41. Witt, O.; Lindemann, R. *Cancer Lett.* **2009**, *280*, 123.
42. Klose, R. J.; Bird, A. P. *Trends Biochem. Sci.* **2006**, *31*, 89.
43. Ooi, S. K. T.; Bestor, T. H. *Cell* **2008**, *133*, 1145.
44. Baylin, S.; Bestor, T. H. *Cancer Cell* **2002**, *1*, 299.
45. Esteller, M. *Oncogene* **2002**, *21*, 5427.
46. Das, P. M.; Singal, R. *J. Clin. Oncol.* **2004**, *22*, 4632.
47. Baylin, S. B. *Nat. Clin. Pract. Oncol.* **2005**, *2*, S4.
48. Brueckner, B.; Lyko, F. *Trends Pharm. Sci.* **2004**, *25*, 551.
49. Kaminskas, E.; Farrell, A.; Abraham, S.; Baird, A.; Hsieh, L.-S.; Lee, S.-L.; Leighton, J. K.; Patel, H.; Rahman, A.; Sridhara, R.; Wang, Y.-C.; Pazdur, R. *Clin. Cancer Res.* **2005**, *11*, 3604.
50. Morphy, R.; Kay, C.; Rankovic, Z. *Drug Discovery Today* **2004**, *9*, 641.
51. Morphy, R.; Rankovic, Z. *J. Med. Chem.* **2005**, *48*, 6523.
52. Remiszewski, S. W. *Curr. Med. Chem.* **2003**, *10*, 2393.
53. Hoshino, O.; Murakata, M.; Yamada, K. *Bioorg. Med. Chem. Lett.* **1992**, *2*, 1561.
54. Nicolaou, K. C.; Hughes, R.; Pfefferkorn, J. A.; Barluenga, S. *Chem. Eur. J.* **2001**, *7*, 4296.
55. Nicolaou, K. C.; Hughes, R.; Pfefferkorn, J. A.; Barluenga, S.; Roecker, A. J. *Chem. Eur. J.* **2001**, *7*, 4280.
56. Godert, A. M.; Angelino, N.; Woloszynska-Read, A.; Morey, S. R.; James, S. R.; Karpf, A. R.; Sufirin, J. R. *Bioorg. Med. Chem. Lett.* **2006**, *16*, 3330.
57. Boehlow, T. R.; Spilling, C. D. *Nat. Prod. Lett.* **1995**, *7*, 1.
58. Boehlow, T. R.; Harburn, J. J.; Spilling, C. D. *J. Org. Chem.* **2001**, *66*, 3111.
59. Carreño, M. C. R.; J.L.G.; Sanz, G.; Toledo, M. A.; Urbano, A. *Synlett* **1997**, 1241.
60. Pfammatter, M. J.; Siljegovic, V.; Darbre, T.; Keese, R. *Helv. Chim. Acta* **2001**, *84*, 678.
61. Nishiyama, S.; Yamamura, S. *Tetrahedron Lett.* **1982**, *23*, 1281.
62. Forrester, A. R. T.; R.H.; Woo, S. O. *J. Chem. Soc., Perkin Trans. 1* **1975**, 2340.
63. Khan, N.; Jeffers, M.; Kumar, S.; Hackett, C.; Boldog, F.; Khramtsov, N.; Qian, X.; Mills, E.; Berghs, S. C.; Carey, N.; Finn, P. W.; Collins, L. S.; Tumber, A.; Ritchie, J. W.; Jensen, P. B.; Lichenstein, H. S.; Sehested, M. *Biochem. J.* **2008**, *409*, 581.
64. Bradner, J. E.; Mak, R.; Tanguturi, S. K.; Mazitschek, R.; Haggarty, S. J.; Ross, K.; Chang, C. Y.; Bosco, J.; West, N.; Morse, E.; Lin, K.; Shen, J. P.; Kwiatkowski, N. P.; Gheldof, N.; Dekker, J.; DeAngelo, D. J.; Carr, S. A.; Schreiber, S. L.; Golub, T. R.; Ebert, B. L. *Proc. Natl. Acad. Sci. U.S.A.* **2010**, *107*, 12617.
65. Balasubramanyam, K.; Swaminathan, V.; Ranganathan, A.; Kundu, T. K. *J. Biol. Chem.* **2003**, *278*, 19134.
66. (a) Souto, J. A.; Conte, M.; Alvarez, R.; Nebbioso, A.; Carafa, V.; Altucci, L.; de Lera, A. R. *ChemMedChem* **2008**, *3*, 1435; (b) Souto, J. A.; Bebedetti, R.; Otto, K.; Miceli, M.; Alvarez, R.; Altucci, L.; de Lera, A. R. *ChemMedChem* **2010**, *5*, 1530; (c) Souto, J. A.; Vaz, E.; Lepore, I.; Pöppler, A.-C.; Franci, J. L.; Alvarez, R.; Altucci, L.; de Lera, A. R. *J. Med. Chem.* **2010**, *53*, 4654.
67. Siedlecki, P.; Boy, R. G.; Musch, T.; Brueckner, B.; Suhai, S.; Lyko, F.; Zielenkiewicz, P. *J. Med. Chem.* **2006**, *49*, 678.
68. Datta, J.; Ghoshal, K.; Denny, W. A.; Gamage, S. A.; Brooke, D. G.; Phiasivongsa, P.; Redkar, S.; Jacob, S. T. *Cancer Res.* **2009**, *69*, 4277.
69. Biel, M.; Wascholowski, V.; Giannis, A. *Angew. Chem., Int. Ed.* **2005**, *44*, 3186.
70. Somoza, J. R.; Skene, R. J.; Katz, B. A.; Mol, C.; Ho, J. D.; Jennings, A. J.; Luong, C.; Arvai, A.; Buggy, J. J.; Chi, E.; Tang, J.; Sang, B. C.; Verner, E.; Wynands, R.; Leahy, E. M.; Dougan, D. R.; Snell, G.; Navre, M.; Knuth, M. W.; Swanson, R. V.; McRee, D. E.; Tari, L. W. *Structure* **2004**, *12*, 1325.
71. Bieliauskas, A. V.; Pflum, M. K. H. *Chem. Soc. Rev.* **2008**, *37*, 1402.
72. McCulloch, M. W. B.; Coombs, G. S.; Banerjee, N.; Bugni, T. S.; Cannon, K. M.; Harper, M. K.; Veltri, C. A.; Virshup, D. M.; Ireland, C. M. *Bioorg. Med. Chem.* **2009**, *17*, 2189.
73. Kim, D. H. S. J.; Kwon, H. J. *Exp. Mol. Med.* **2007**, *39*, 47.
74. Ahn, M. Y.; Jung, J. H.; Na, Y. J.; Kim, H. S. *Gynecol. Oncol.* **2008**, *108*, 27.
75. Richon, V. M.; Sandhoff, T. W.; Rifkind, R. A.; Marks, P. A. *Proc. Natl. Acad. Sci. U.S.A.* **2000**, *97*, 10014.
76. Mai, A.; Massa, S.; Rotili, D.; Cerbara, I.; Valente, S.; Pezzi, R.; Simeoni, S.; Ragna, R. *Med. Res. Rev.* **2005**, *25*, 261.
77. Furumai, R.; Matsuyama, A.; Kobashi, N.; Lee, K. H.; Nishiyama, M.; Nakajima, H.; Tanaka, A.; Komatsu, Y.; Nishino, N.; Yoshida, M.; Horinouchi, S. *Cancer Res.* **2002**, *62*, 4916.
78. Xiao, J. J.; Byrd, J.; Marcucci, G.; Grever, M.; Can, K. K. *Rapid Commun. Mass Spectrom.* **2003**, *17*, 757.
79. Wang, D.; Helquist, P.; Wiest, O. *J. Org. Chem.* **2008**, *72*, 5446.
80. Nishino, N.; Jose, B.; Okamura, S.; Ebisusaki, S.; Kato, T.; Sumida, Y.; Yoshida, M. *Org. Lett.* **2003**, *5*, 5079.
81. Nishino, N.; Shivashimpi, G. M.; Soni, P. B.; Bhuiyan, M. P. I.; Kato, T.; Maeda, S.; Nishino, T. G.; Yoshida, M. *Bioorg. Med. Chem.* **2008**, *16*, 437.
82. Bach, R. D.; Dmitrenko, O.; Thorpe, C. J. *Org. Chem.* **2008**, *73*, 12.
83. Rautio, J.; Kumpulainen, H.; Heimbach, T.; Oliyai, R.; Oh, D.; Järvinen, T.; Savolainen, J. *Nat. Rev. Drug Disc.* **2008**, *7*, 255.
84. Mai, A.; Cheng, D.; Bedford, M. T.; Valente, S.; Nebbioso, A.; Perrone, A.; Brosch, G.; Sbardella, G.; De Bellis, F.; Miceli, M.; Altucci, L. *J. Med. Chem.* **2008**, *51*, 2279.
85. Li, J. W. H.; Vederas, J. C. *Science* **2009**, *325*, 161.
86. Newman, D. J. *J. Med. Chem.* **2008**, *51*, 2589.
87. Molinski, T. F.; Dalisay, D. S.; Lievens, S. L.; Saludes, J. P. *Nat. Rev. Drug Disc.* **2009**, *8*, 69.
88. Kotoku, N.; Tsujita, H.; Hiramatsu, A.; Mori, C.; Koizumi, N.; Kobayashi, M. *Tetrahedron* **2005**, *61*, 7211.
89. Knapp, S.; Amorelli, B.; Darout, E.; Ventocilla, C. C.; Goldman, L. M.; Huhn, R. A.; Minnihan, E. C. *J. Carbohydr. Chem.* **2005**, *24*, 103.
90. Frisch, M. J.; G. W. T.; Schlegel, H. B.; Scuseria, G. E.; Robb, M. A.; Cheeseman, J. R.; Montgomery, Jr., J. A.; Vreven, T.; Kudin, K. N.; Burant, J. C.; Millam, J. M.; Iyengar, S. S.; Tomasi, J.; Barone, V.; Mennucci, B.; Cossi, M.; Scalmani, G.; Rega, N.; Petersson, G. A.; Nakatsuji, H.; Hada, M.; Ehara, M.; Toyota, K.; Fukuda, R.; Hasegawa, J.; Ishida, M.; Nakajima, T.; Honda, Y.; Kitao, O.; Nakai, H.; Klene, M.; Li, X.; Knox, J. E.; Hratchian, H. P.; Cross, J. B.; Bakken, V.; Adamo, C.; Jaramillo, J.; Gomperts, R.; Stratmann, R. E.; Yazyev, O.; Austin, A. J.; Cammi, R.; Pomelli, C.; Ochterski, J. W.; Ayala, P. Y.; Morokuma, K.; Voth, G. A.; Salvador, P.; Dannenberg, J. J.; Zakrzewski, V. G.; Dapprich, S.; Daniels, A. D.; Strain, M. C.; Farkas, M. L.; Malick, O.; D. K.; Rabuck, A. D.; Raghavachari, K.; Foresman, J. B.; Ortiz, J. V.; Cui, Q.; Baboul, A. G.; Clifford, S.; Cioslowski, J.; Stefanov, B. B.; Liu, G.; Liashenko, A.; Piskorz, P.; Komaromi, I.; Martin, R. L.; Fox, D. J.; Keith, T.; Al-Laham, M. A.; Peng, C. Y.; Nanayakkara, A.; Challacombe, M.; Gill, P. M. W.; Johnson, B.; Chen, W.; Wong, M. W.; Gonzalez, C.; Pople, J. A. *Gaussian, Pittsburg*: 2004.
91. Bayly, C. I.; Cieplak, P.; Cornell, W. D.; Kollman, P. A. *J. Phys. Chem.* **1993**, *97*, 10269.
92. Cornell, W. D.; Cieplak, P.; Bayly, C. I.; Gould, I. R.; Merz, K. M.; Ferguson, D. M.; Spellmeyer, D. C.; Fox, T.; Caldwell, J. W.; Kollman, P. A. *J. Am. Chem. Soc.* **1995**, *117*, 5179.
93. Rodríguez-Barríos, F.; Pérez, C.; Lobatón, E.; Velázquez, S.; Chamorro, C.; San-Félix, A.; Pérez-Pérez, M. J.; Camarasa, M. J.; Pelemans, H.; Balzarini, J.; Gago, F. *J. Med. Chem.* **2001**, *44*, 1853.
94. Morris, G. M.; Goodsell, D. S.; Halliday, R. S.; Huey, R.; Hart, W. E.; Belew, R. K.; Olson, A. J. *J. Comput. Chem.* **1998**, *19*, 1639.
95. Morris, G. M.; Goodsell, D. S.; Huey, R.; Hart, W. E.; Halliday, S.; Belew, R.; Olson, A. J.; AutoDock, 3.0 ed. La Jolla, CA, 1999.
96. Goodford, P. J. *J. Med. Chem.* **1985**, *28*, 849.
97. Åqvist, J. *J. Phys. Chem.* **1990**, *94*, 8021.
98. Jorgensen, W. L.; Chandrasekhar, J.; Madura, J. D. *J. Chem. Phys.* **1983**, *79*, 926. <http://amber.scripps.edu/doc8>.
99. Rychkaert, J. P.; Cicotti, G.; Berendsen, H. J. C. *J. Comput. Phys.* **1977**, *23*, 327.
100. Nebbioso, A.; Clarke, N.; Voltz, E.; Germain, E.; Ambrosino, C.; Bontempo, P.; Alvarez, R.; Schiavone, E. M.; Ferrara, F.; Bresciani, F.; Weisz, A.; de Lera, A. R.; Gronemeyer, H.; Altucci, L. *Nat. Med.* **2005**, *11*, 77.
101. Scognamiglio, A.; Nebbioso, A.; Manzo, F.; Valente, S.; Mai, A.; Altucci, L. *Biochem. Biophys. Acta* **2008**, *1783*, 203.
102. Altucci, L.; Rossini, A.; Raffelsberger, W.; Reitmaier, A.; Chomienne, C.; Gronemeyer, H. *Nat. Med.* **2001**, *7*, 680.